International Pipeline Conference - ASME 1996

IPC1996-1843

RESIDUAL STRENGTH OF 48-INCH DIAMETER CORRODED PIPE DETERMINED BY FULL SCALE COMBINED LOADING EXPERIMENTS

Stephen C. Grigory
Southwest Research Institute
P. O. Drawer 28510
San Antonio, TX 78228-0510

Marina Q. Smith
Southwest Research Institute
P.O. Drawer 28510
San Antonio, TX 78228-0510

ABSTRACT

To provide a data base for the confirmation of computational and classical residual strength analyses of corroded pipelines subjected to combined loads, full scale experiments of 48-inch diameter pipe sections with artificial corrosion were conducted. Design of the experiments was guided by the prerequisite of testing pipe sections in full scale such that subsequent corrections for the uniform depth and extent of the degraded region, and *D/t* ratios were not required. The testing and analysis procedures were progressively developed through three distinct phases of the program: 1) one *proof of concept* experiment performed on smaller diameter pipe with artificial corrosion subjected to internal pressure and axial bending, 2) five 48-inch diameter pipe tests, each with artificial corrosion, subjected to internal pressure and axial bending, and 3) eight 48-inch diameter pipe tests, each with artificial corrosion subjected to pressure, axial bending, and axial compression. Combined loading on the test specimens followed a predetermined path until failure by either rupture or global buckling occurred, while the elastic-plastic load-deflection and large strain behavior was recorded. The uniform depth, axial length, and circumferential length of the degraded region were selected to represent commonly observed general corrosion dimensions found among in-service pipelines, with the maximum and minimum extents reflecting the typical wall loss characteristics at the girth and seam weld locations. The pipe behavior during the experiments and analyses was ultimately modeled and verified by an elastic-shell model capable of defining failure pressure and curvature for a corroded pipe subjected to combined service loads.

This paper presents details on the test procedures, specimen preparation and design, and complex data acquisition techniques utilized in the generation of required global and location response information. In addition, significant experimental results from the program which enabled the development and validation of a new procedure for the assessment of corroded pipes under combined loads are reviewed.

INTRODUCTION

When corrosion damage in the form of wall loss (referred to in this program as a corrosion patch in the context of a cabbage patch) is discovered by a pigging or excavation operation, a replace/repair/ignore decision must be made. This decision hinges crucially on a prediction of the failure pressure of the corroded pipe. Above all else, because environmental safety is paramount, the failure pressure that is predicted for the observed damage must be reliable and readily obtainable. But at the same time, unnecessary field maintenance operations should not be performed—not only to avoid unnecessary expenses and curtailment of service, but also to prevent the possibility of additional damage that sometimes occurs in field operations. Thus, the prediction must be accurate without being grossly conservative, and should not require a time consuming analysis procedure.

The current and potential new ASME B31G guidelines satisfy these requirements for most existing pipelines. However, because the present guidelines are drawn from methods that are both empirically based and have a somewhat limited range of applicability, there are pipeline service conditions for which they may not be entirely appropriate. These include damage regions having a large circumferential dimension, multiple nearby interacting discrete damage zones, damage zones at or near weldments, and combined loading conditions.

This study was aimed at providing a theoretically-sound technology for a 48-inch pipeline, that will ultimately be adapted to pipelines in general, by conducting integrated research including (1) full-scale pipe burst experimentation, (2) finite element analyses (FEA), and (3) an engineering model for field use embodied in a PC program. Tests and analyses were conducted to delineate the effects of corrosion patch dimensions on the failure mode. Preliminary work [1] (Phase 1 of the study) consisted of a proof of concept test on a 20-inch (51 cm) diameter, X52 steel pipe with simulated corrosion metal loss under a combination of internal pressure and axial bending. Phase 2 of the study consisted of tests and analyses of full scale 48-inch (1.22 m) diameter X65 steel pipes

with simulated corrosion patches loaded in bending and internal pressure. Axial compression was added in Phase 3 of the program to simulate the compressive loads on this pipeline which occur when the line is layed in cold weather and then loaded with hot product. This paper discusses the full-scale testing. The FEA procedures, detailed information on the engineering model and PC program is contained in reference [2].

SPECIMEN DESIGN

Thirteen specimens were fabricated from 48-inch (1.22 m) outside diameter, 0.462-inch (11.7 mm) wall, API 5L X65 steel pipes. The test section was 12-feet (3.7 m) long with the overall length of the specimen being about 60-feet (18.3m) as may be seen in the photograph and sketch in Figure 1. The balance of the specimen length consisted of two reinforced sections of 48-inch (1.22 m) diameter, X70 pipe with a 0.562-inch (14.3 mm) thick wall that were reused on each test. Simulated corrosion patches with uniform depth were machined on each pipe specimen. Because it was not known whether corrosion in the nominal tension or the nominal compression side of the pipe would be more detrimental, identical corrosion patches were machined on both sides of the pipe in the plane of bending. Tests 1 through 9 were conducted with symmetrically oriented patches thereby providing the failure process equal opportunity to manifest itself. However, the practice of grinding identical patches on the compressive as well as the tensile side of the pipe specimen was discontinued when these tests confirmed that the rupture failure occurred predominantly in the patch on the compression side. Table 1 gives patch dimensions and locations for each test. The dimensions and locations of the corrosion patches used on each test are also shown in Figure 2.

Machined Simulated Corrosion

Simulated corrosion patches were machined on the outside surface of each specimen in the plane of bending. The patches were uniform in depth to produce a test specimen that could be simulated easily for the finite element analysis and was aminable to strain gage instrumentation.

Some specimens had patches machined on both sides of the pipe and others had specimens machined on one side only as noted in the descriptions of the specimens in the previous section. The jig used to grind the simulated corrosion areas on the 48-inch pipe was designed to provide good control of the grinding operation and to hold a close tolerance of the patch depth. One to two weeks were required to grind the patches on a single pipe.

EXPERIMENTAL FACILITIES

Frame Design

A photograph of the test frame, which was constructed at SwRI, and a sketch showing overall dimensions is presented in Figure 1. Axial loads up to 4-million pounds (17.8 MN) compression force, bending loads up to 6-million foot-pounds (8100 kN-m) and internal pressure well beyond the working pressure of 950-psig (65.5 bar) could be applied simultaneously. Lateral displacement is deflection controlled and deflections to eight inches (203 mm) are possible with load cylinders in push or pull mode. Shims were used to obtain deflections up to 18 inches when load conditions were such that buckling did not occur within the 8-inch stroke of the cylinder.

Applied Loads

As may be seen in Figure 1, the bending frame is independent of the axial load frame. Total bending moment in the specimen has three sources: (1) dead weight, (2) lateral loads on the specimen and (3) axial load when the pipe is deflected.

Strains in the specimen due to dead weight of the water are measured before each test when the specimen is filled. The strains in the specimen from the weight of the steel pipe cannot be determined after the pipe is in the test frame. While the pipe was still in the shop supported by rollers at each end, a single channel strain gage readout was used to take reading on the four gages installed on the gross section of the test section (half way between the patch and the end of the test section) with the gages located top and bottom and oriented in the axial direction. Strain gage readings were taken, then the pipe was rotated and a second set of readings were taken. As a gage on the top of the pipe is rotated 90°, the strain in the steel changes from maximum compression to zero at the neutral axis and then to maximum tension as the gage is rotated to the 180° position. This procedure yields a stress from double the weight of the pipe. The pipe was supported with the rollers at the end of the pipe on the 4-inch thick plates. A ratio of pipe dead weight to water dead weight was established at the selected gages. This ratio was used to calculate the steel weight effect at all strain and displacement locations based on the weight of water measurements made before each test. The ratio of steel weight to water weight is valid at each location because both are essentially evenly distributed loads.

The maximum axial compressive stress that was to be applied to a pipe specimen on specimens 7 through 13 was the stress caused by thermal expansion of a 135°F temperature rise. (The pipe was installed at ambient conditions as low as 5°F (-15°C) and the product may be as hot as 140°F (60°C)). In addition to the load required to simulate the thermal stress, the load to offset the tensile load from internal pressure thrust less the tensile load from the Poisson's ratio effect in a buried pipe due to internal pressure, would be added during a test.

In the ground, the pipe is constrained and cannot expand axially. As a result, compressive stresses result. For example, if the pipe temperature is 5°F when installed and hot oil with a temperature of 140°F is pumped through the line, the steel temperature differential is 135°F. A piece of pipe on the surface would expand freely, increase in length and no stress would be created in the pipe. However, in the ground the pipe cannot expand and a stress builds up in the heated pipe equal to stress caused by a force that would be required to compress the freely expanded pipe back to its original length before it was heated. This example is illustrated in Figure 2. The thermal load is calculated by multiplying the coefficient of thermal expansion, 6.5×10^{-6}, by the temperature rise, 135°F and by the steel area of the pipe, 69-in^2. The axial load due to restraint of thermal expansion was calculated at 1.816 million pounds.

A second axial stress found in a buried pipe is a tensile stress caused by the Poisson's ratio effect from internal pressure. The concept of Poisson's ratio is best illustrated by stretching a bar a distance, *d*. The bar will shrink in directions 90° to the direction of stretch. For steel the amount of shrinkage is equal to 0.3 times the amount of stretch, *d*. As in thermal expansion, if the shrinkage is restrained, a tensile stress will build up equal to that caused by the force required to stretch the steel back to its original shape. An example of Poisson's ratio effect on the buried pipe subjected

to internal pressure is also illustrated in Figure 2. For the 48-inch pipe subjected to a test pressure of 1500 psig (103 bar) internal pressure, the test load to simulate the corresponding tensile stress in a buried pipe due to Poisson's ratio is 1.6 million pounds (7.12 MN).

The third load component that must be applied during the test is the compressive force required to offset the tensile force that results from internal pressure on the closed ends of the test specimen. The buried pipe has no closed ends and the loads created at bends in the buried pipe are transferred directly to the ground. The external axial load required to offset internal pressure is simply the internal area of the pipe, 1741-in^2, times the pressure. The maximum pressure for design purposes was considered to be the maximum pressure achieved in Phase II or about 1500 psig. The corresponding external compression load at 1500 psig is 2.65 million pounds.

The total load that could potentially be applied was taken to be 2.82 million pounds. The maximum axial load capacity of the test frame was designed to be 4 million pounds. The maximum axial load applied to any specimen was 2.8 million pounds (Specimen 9).

Several curves showing the loads discussed above were generated to assist the design of the test facility and verify concepts. Figure 3 was generated to show the axial stress in a buried pipe as pressure is increased with a constant temperature differential of 135°F. The curve was generated based on the assumption that the temperature differential existed before internal pressure was applied. The net compression load on the pipe then decreases as internal pressure is increased because the Poisson's ratio effect on the pipe causes a tensile stress. However, there is a tensile load caused by internal pressure acting on the closed ends of the specimen. This tensile load must be offset by a compressive load during the test because in does not exist on the pipe in the ground. The applied compression load required to offset internal pressure load is larger than the tensile load from the Poisson's effect. Therefore, the applied compression load on the test specimen increases even though the net compression load on the pipe is decreasing.

Figure 4 is a plot of axial stress versus internal pressure in a buried pipe with a family of curves representing different values of temperature differential. The curves were generated to show the equivalent conditions in a buried pipe as internal pressure is increased during a test if the axial stress were held constant. Axial stress was held at zero during Tests 1, 2 and 3 by applying just enough axial compressive load to offset the axial tensile force from internal pressure. The zero line for axial stress is traced across the graph to show the equivalent pipeline temperature differential for any given pressure. Tests 1, 2, and 3 were performed to provide data for confirmation of the predictive capabilities of the computer program for simple stress states and did not represent actual field conditiions.

Instrumentation

Fifty channels of strain gage instrumentation were installed on each pipe to determine the strain distribution on the corrosion patch and on the gross section of the pipe. The strain gages in the patch were high elongation gages with a potential strain measurement capability of up to 15%. Fourteen linear potentiometers were used on each test to determine the deflection at the load points, the center and the ends of the pipe. Pressure transducers were installed on the load cylinders so that load could be recorded as a function of cylinder pressure. A pressure transducer was installed on the pipe so that internal pressure could be recorded. Data logging of the strain gages was performed with high speed signal conditioners that could scan 50 channelsat 20 times per second. This feature was used when pipe burst was eminent. Normally, the channels were scanned once and recorded at each load increment.

ARTIFICIALLY CORRODED PIPE EXPERIMENTATION

Thirteen experiments were performed on 48-inch (1.22 m) outside diameter, 0.462-inch (11.7-mm) wall, API 5L X65 steel pipes. Of these, the first five tests were performed under the capped-end condition without axial compression. Moderate to high longitudinal compression was applied for the remaining tests to simulate the constrained thermal expansion and effect encountered in a buried pipe subjected to internal pressure. Each of the pipes were subjected to four-point bending in conjunction with internal pressurization. The lateral loads actually reacted to a signal from a linear potentiometer so that bending was deflection controlled. Applied longitudinal compression was load controlled. Axial and lateral loads automatically responded to electronically set values and were applied proportionally as loads and deflections were increased.

The applied loads simulated possible loads on buried portions of the Trans-Alaskan Pipeline. Bending loads are due to settlement and axial loads are the sum of the tension from Poisson's effect and compression from thermal expansion. The pipe is assumed to be restrained by friction of the soil. When the pipe expands from internal pressure the Poisson's effect causes a tensile stress in the pipe. The pipe was installed at ambient conditions as low as 5°F (-15°C) and the product may be as hot as 140°F (60°C), creating a high compressive load.

Test 2 and Test 5 are the only set of tests where the corrosion patch on the tension side ruptured, with the crack running in a circumferential direction. In fact, Test 5, which is a replicate of Test 2, was conducted to confirm the repeatability of the tension-side failure. This tension failure mode is a result of a long, narrow circumferential corrosion patch and a net axial tensile stress (internal pressure acting against capped ends). All other rupture failures were observed to occur within the corrosion patch on the compression side of the pipe, with the crack running in the axial direction.

In an attempt to precipitate a rupture on the tension side of a pipe with a single corrosion patch, test specimen 10 was designed with a single corrosion patch on the tension side of the pipe subjected to high axial compression. However, the pipe in this test failed in a bending collapse mode before rupture could initiate. The remaining tests (Tests 11 through 13) were conducted with a single corrosion patch on the compression side subjected to high axial compression. In an effort to assess the remaining strength of a corroded pipe after wrinkling has occurred, the pipe in Test 13 was deflected until peak moment was reached (listed as 13a), and then pressurized to failure (listed as 13b).

The loading applied on the pipe specimen typically consisted of three steps in tests 1 through 5. During step one, internal pressure was ramped up to the operating pressure for the pipe, approximately 1000 psi (6.9 MPa). Step two consisted of applying four-point bending to the pipe up to a specified transverse deflection,

typically just enough to cause outer fiber yield in the nominal section, while holding the internal pressure and axial compression constant. Finally, in step three, the pipe was pressurized to failure. In tests 6, 7 and 8 an axial load was applied to offset the thrust from internal pressure amd maintain zero axial stress. In addition, bending was applied first in test 6 then pressurized to failure with appropriate change in axial compressive load while holding the transverse pipe deflection constant.

Axial load was applied first in tests 9 through 13 to simulate the existing thermal stress in the pipe. While the test procedure was altered by circumstances arising in some tests, the loading sequence generally consisted of three steps described above. First, the pipe was pressurized to an operating pressure of 950 psi (6.55 MPa). Second, the pipe was loaded in four point bending until an additional 0.4% strain in the nominal wall thickness (i.e., in addition to that arising from the weight of the pipe and its contents) was reached on the tension side. Third, the pipe was further pressurized until burst occurred unless bending collapse occured during the bending load application. Strain gages were installed on the simulated corrosion patches and on the nominal section of the 12-foot (3.7 m) test pipe at locations guided by pre-test finite element analyses. The patch dimensions and failure mode for each specimen are given in Table 1. Typical ruptures are shown in Figure 6. Note that in Table 1 the Pressure and bending moment at failure do no necessarily correspond to the final data point in the graphs of bending versus internal pressure for each test. This is because it was necessary to pick the data point that corresponed to eleastic instabliity to match the definition of failure used in the FEA analysis.

TEST RESULTS

Specimens 1 through 5

Tests of Specimens 1 through 5 were valuable in calibrating the computer model but, in the absence of thermally induced axial compressive loads, did not sufficiently represent the load conditions on buried portions of the pipe line under study. Therefore, most of this paper is dedicated to tests 6 through 13 of this test series. One may note in Table 1,by comparing the failure loads of tests 2, 4 and 5 with comparable specimens subject to axial load, that in the absence of high compressive loads, the pipe will sustain much higher bending loads.

Specimen 6 and 7

Specimens 6 and 7 were tested to check the effects if any of load sequence on failure pressure and load. Both specimens had identical simulated corrosion patches 1/2 the wall thickness in depth, 30-inches along the axis and 6-inches in the circumferential direction. Duplicate patches were machined top and bottom. The maximum bending displacement for the test was established in advance for Specimen 6 by analysis. Specimen 6 was then pressurized to failure. An axial load was applied to maintain zero axial stress as pressure was increased (internal pressure creates a tensile axial force on the test specimen and an external compressive load was applied to offset this force. (See Figure 4). The internal pressure at which Specimen 6 failed was applied to Specimen 7 with axial load applied to maintain zero axial stress. Bending load was then applied to Specimen 7 until failure occurred.

Specifically, bending load was applied to Specimen 6 until the load point displacement was 2.5-inches (about 3-inches at the center). Pressure was increased until failure occurred at 958-psig. Specimen 7 was pressurized to 960-psig and bending applied until rupture occurred. Moment versus internal pressure curves for Specimens 6 and 7 are shown in Figure 7 These curves demonstrate that loading sequence does not affect results within the parameters chosen for these tests.

Specimen 8

Specimen 8 was tested to determine the effect of a moderate axial compressive stress on the failure mode of a long narrow circumferential corrosion patch. In Phase II tests of two specimens with a 6-inch ×30-inch patch resulted in a failure on the tension side of the bent pipe whereas all other specimens failed on the compression side of the pipe. Also, the pretest analysis predicted a failure on the compression side. A moderate compressive load, sufficient to maintain zero axial stress, was applied to the pipe as pressure was increased but otherwise the test was a repeat of Tests 2 and 5 in Phase II. Internal pressure was applied to 950-psig with axial load sufficient to maintain zero axial stress at the neutral axis. Bending load was applied until the load point displacement was 3-inches. Then, internal pressure was applied while maintaining zero axial stress until the pipe burst. The depth of the simulated corrosion patch on Specimen 8 was 1/2 the wall thickness. The moment versus internal pressure curve for Specimen 8 is shown in Figure 8.

Specimen 9

Specimen 9 was tested to determine the effect of a high compressive load on failure mode and failure load magnitude on a pipe with a long narrow axial patch. Two patches, 180° apart in the plane of bending, were 30 inches axial ×6-inches circumferential ×1/2 the wall thickness. An axial compressive load that simulates thermal expansion from a temperature increase of 135°F was applied first. Internal pressure with proportional axial load was increased to 400 psig. Bending loads were applied until the load points deflected 1.5 inches. Then internal pressure with proportional axial load was increased until the pipe burst. The moment versus internal pressure curve is shown in Figure 8.

Specimens 10

Specimen 10 was tested to determine the effect of a high compressive load on failure mode and failure load magnitude on a pipe with a long narrow circumferential patch. The simulated corrosion patch was 6 inches axial ×30 inches circumferential × 1/2 wall thickness in depth. One patch on the tension side only, in the plane of bending, was machined on the pipe. The loading sequence and initial axial load magnitudes for Specimen 10 was the same as that applied to for Specimen 9. Internal pressure of 800 psig was then applied with a proportional axial load to simulate buried pipe loads. A bending load was applied to produce about 1.5 inches deflection at the load points. Internal pressure and proportional axial load were then applied until failure occurred. The moment versus internal pressure curve is shown in Figure 10.

Specimen 11

Specimen 11 was tested to study the effect on size of corrosion areas with a circumferential-to-axial ratio of 1.5:1. One large patch of 30 inches axial ×45 inches circumferential × 0.15t wall thickness in depth was machined on the compression side of the pipe. The

load sequence was the same as that for Specimen 10. The axial load to simulate 135°F temperature differential was applied first. The pipe was then pressurized to 1000 psig with proportional axial load to simulate buried pipe loads. A bending load was applied to produce about 1.5 inches deflection at the load points. Internal pressure and proportional axial load were then applied until failure occurred. The moment versus internal pressure curve is shown in Figure 11.

Specimen 12

Specimen 12 was tested to obtain a rupture at low pressure and high bending moment for computer model verification. A 6-inch axial ×30-inch circumferential ×1/2t deep patch was machined on the compression side only. The test sequence was low internal pressure (150 psig), bending until the center of the pipe deflected to 4.5 inches and then increase internal pressure to failure. The axial load on the pipe was adequate to simulate Poisson's effect and to offset axial thrust from internal pressure. The simulated temperature differential was zero. The moment versus internal pressure curve is shown in Figure 12.

Specimen 13

The Specimen 13 test was very similar to test 9 but was intended to result in a low pressure rupture. A 30-inch axial × 6-inch circumferential ×1/2t deep patch was machined on the compression side only. Axial load to simulate 135°F temperature differential was applied first. Internal pressure was increased to 400 psig with a proportional axial load. Bending loads were applied until the center of the pipe deflected four inches (3.25 inches at the load point) which was sufficient to cause bending collapse in a laterally unsupported pipe. Deflection was held constant as internal pressure, with proportional axial load, was increased until the pipe burst. The moment versus internal pressure curve is shown in Figure 13 The failure of Specimen 13 was very similar to Specimen 9. However, the bending moment on Specimen 13 was purposely increased until bending collapse was imminent as may be seen in Figure 13, where the moment reaches a peak and then decreases with no increase in pressure. Deflection is held constant by the lateral hydraulic cylinders so that the load to maintain that deflection must decrease if collapse (the ability of the pipe to support a bending load) has occurred. Had the deflection not been held constant by the cylinders the pipe would have buckled. This is very similar to a pipeline with high loads that settles locally to the point of collapse but the soil conditions are such that settlement does not continue.

For Test 13 the bending collapse is considered a failure point and is designated in Table 1 as test 13. Pressure was then increased until the pipe burst and this failure is designated test 13a.

DISCUSSION

Thirteen full-scale 48-inch (1.22m) pipes with artificially induced corrosion simulation regions were tested under combined pressure and axial bending and compressive loads. In nine experiments, two symmetrically located artificial corrosion patches were examined to ascertain that for patches of approximately equal circumferential and axial dimension, failure is predominantly produced on the nominally compressive side of the pipe irrespective of the presence of axially compressive loading. In contrast, for the pair of replicated tests in which the axial dimension of the corrosion patch was much less than the circumferential dimension, and in the absence of axial compression, failure occurred in the nominally tension side of the pipe in the form of a crack that propagated in the circumferential direction. Bending collapse of the pipe was produced when corrosion patches were of large circumferential dimension and high axial compressive loads were introduced.

While it was only possible to admit a small range of corrosion patch dimension to the experimental program, it nonetheless seems clear that at least three competing failure modes exist in combined pressure, bending, and axial loading conditions. These are:

- a hoop stress dominated axial direction rupture that occurs on the nominally compressive side of the pipe, or
- an axial stress dominated circumferential direction rupture that occurs on the nominally tension side of the pipe, or
- a bending, or global collapse due to a loss of bending stiffness which initiates in the reduced cross section of the pipe.

A competition between different failure mechanisms exists with the dimension of the corrosion region and magnitude of axial stresses strongly influencing the mode that ultimately produces failure.

A considerable volume of strain and displacement data were obtained on this program and publication in a paper is not feasible. However, if interested parties obain written permission from the Alyeska Pipeline Service Company, the author will supply this information in spreadsheet form at no charge.

Additional experimental data are available on tests of 48-inch diameter pipe (with no known defects) that were conducted to prior to construction of the pipeline. [3]

CONCLUSIONS

For economic reasons it was only possible to test a small range of corrosion patch dimensions and only few load cominations could be considered in the experimental program. However, it is intended that an analyses can be carefully calibrated and verified against these full-scale experiments for subsequent use in performing less costly surrogate experiments on a wide range of defect geometries and loading conditions. Because field-useable methods are also needed, simpler approaches have been and can be further developed which are based on experimental and FEA generated data which allow for the broadening and refinement of current guidelines, [2, 4].

ACKNOWLEDGEMENTS

The work described in this paper was performed at the Southwest Research Institute in a project supported by the Alyeska Pipeline Service Company (APSC). Contributing to that project were E. L. Von Rosenberg of Materials Welding Technology; Dr. James A. Maple of J. A. Maple & Associates; and Mr. Gary G. Simmons, Mr. Bill Flanders, and Mr. Mark Anderson of APSC. The contributions of Mel Kanninen, project manager until his retirement, are also greatfully acknowledged.

REFERENCES

1. Kanninen, M. F., A. E. Crouch, H. Kwun, S. C. Grigory, G. K. Wolfe, S. Roy, and R. J. Dexter, 1991, "Development of Methodologies for Determining the Integrity of Corroded Pipelines," Southwest Research Institute Phase I Final Report to Alyeska Pipeline Service Company.
2. Roy, S., Kanninen, M. F., Grigory, S. C., Couque, H. R. A., Smith, M. Q., 1994, "The Development of Methodologies for Determining the Integrity of Corroded Pipelines," Southwest Research Institute Phase III Final Report to Alyeska Pipeline Service Company.
3. Bouwkamp, J. G. and R. M. Stephen, "Full-Scale Studies on the Structural Behavior of Large Diameter Pipes Under Combined Loading," University of California at Berkely, Report No. UC-5ESM 74-1 to Alyeska Pipeline Service Co., January 1974.
4. Grigory, Steve C., Smith, Marina Q., Kanninen, Melvin F., and Roy, Samit, 1996, "The Development of Methodologies for Evaluating the Integrity of Corroded Pipelines Under Combined Loading - Part 1: Experimental Testing and Numerical Simulations," Proceedings for Energy Week '96, Ppielines, Terminals, and Storage Conference, Houston, Texas.

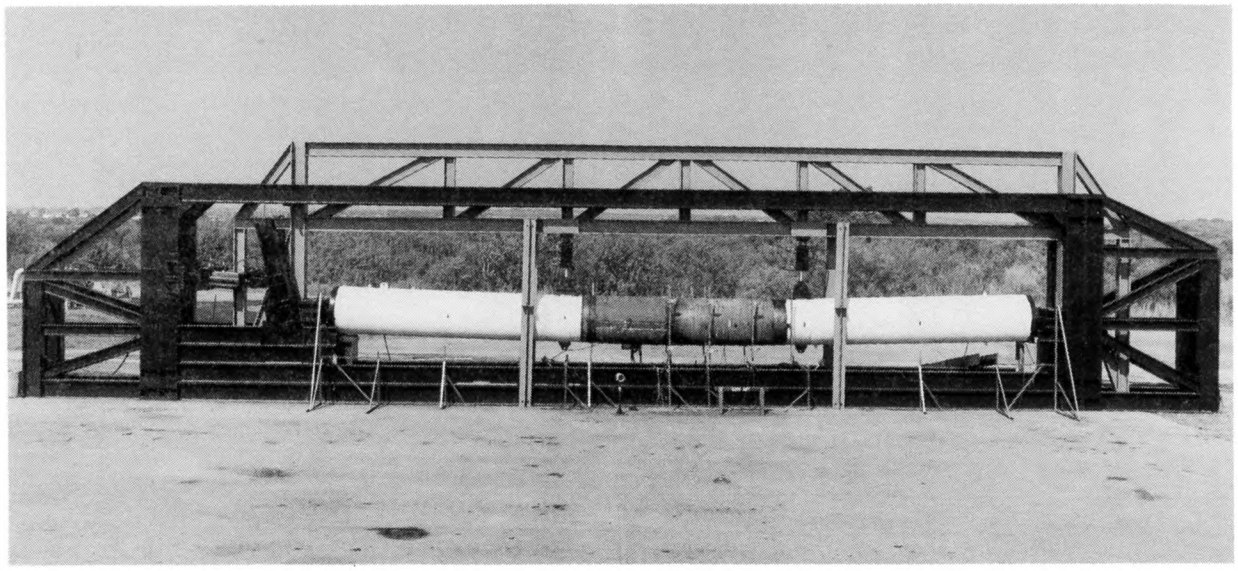

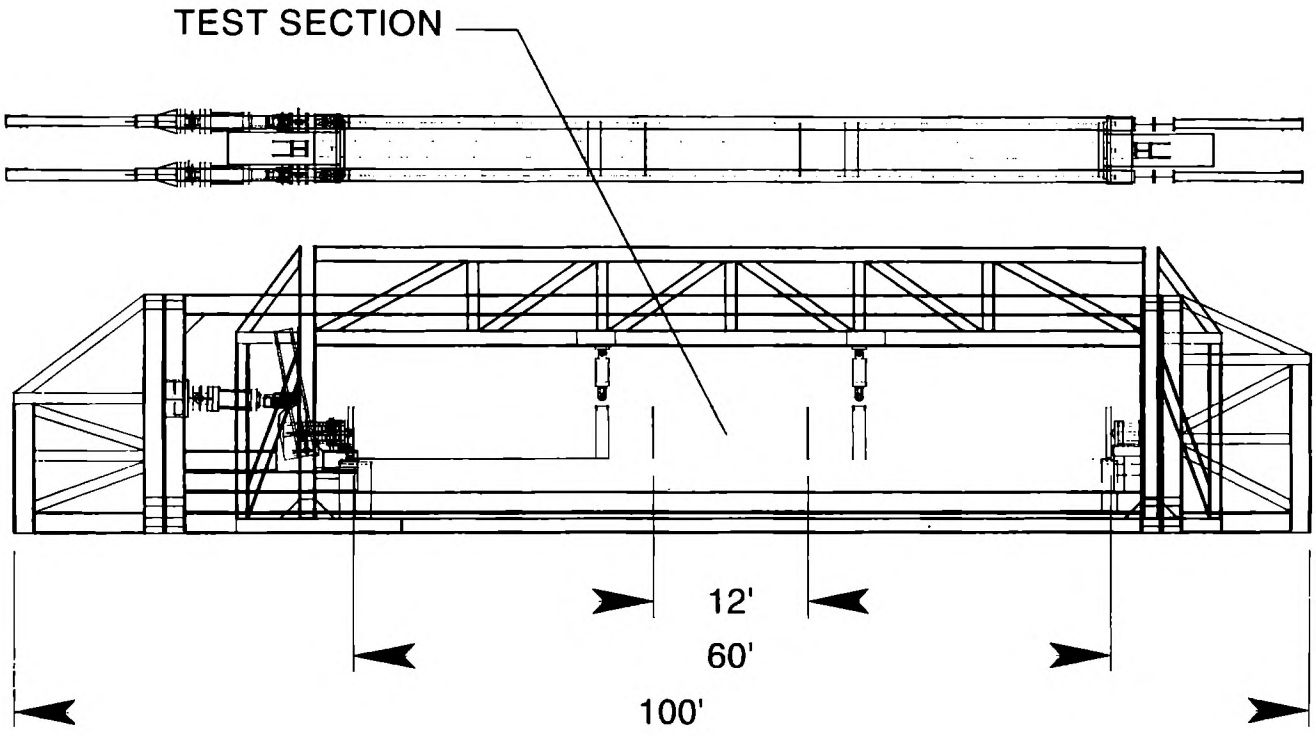

Figure 1: Test Frame for Axial Compression, Bending, and Internal Pressure.

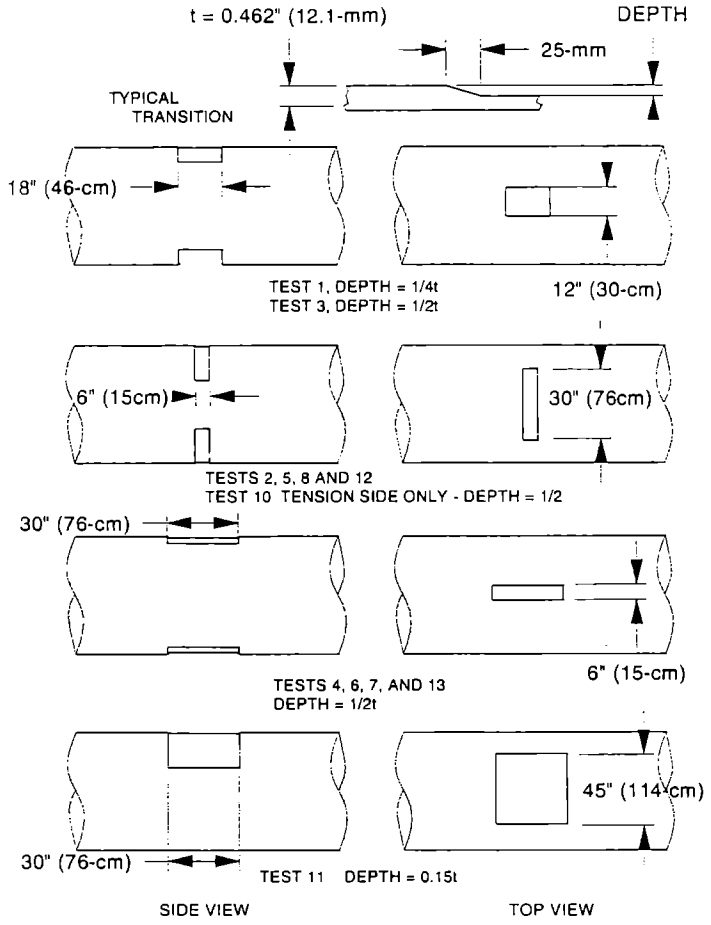

Figure 2: Simulated Corrosion Patch Designs

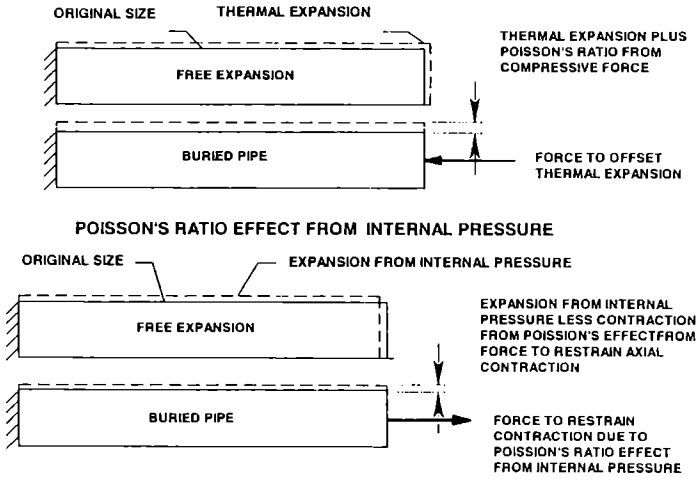

Figure 3: Illustration of Thermal Load and Load From Poisson's Ratio Effect

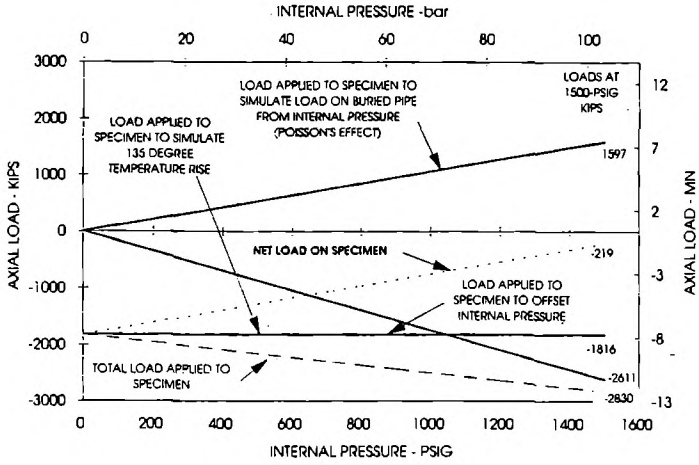

Figure 4: Axial Loads to Simulate 135°F Temperature Differential and Poisson's Effect from Pressure

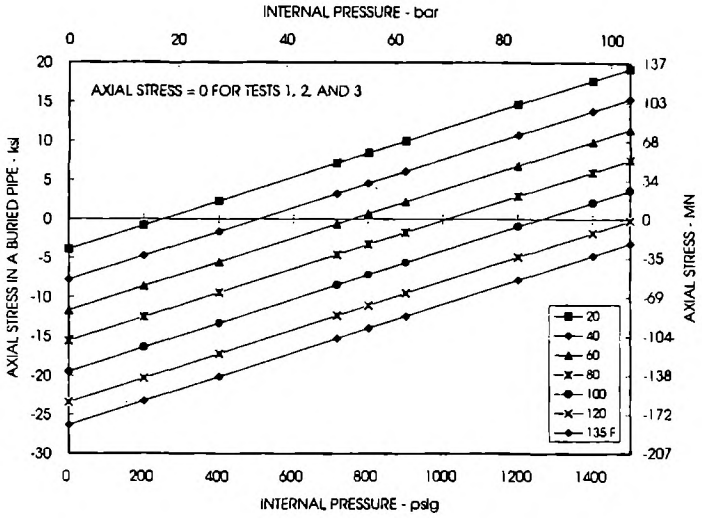

Figure 5: Family of Curves to Show Simulated Temperature Differential for Fixed Axial Stress

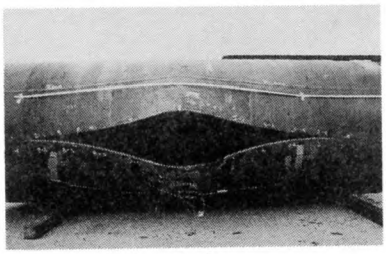

Typical of Phase 3 Tests 7, 8, and 12

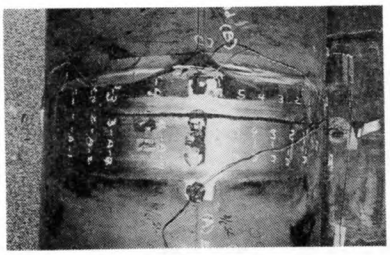

Phase 2 - Tests 2 and 5

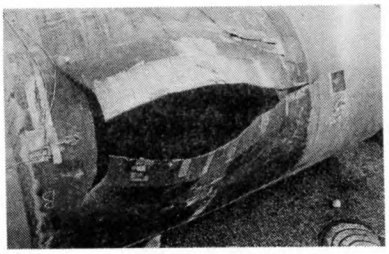

Phase 2 - Test 4
Typical of Phase 3 Tests 6, 9, and 13

Figure 6: Typical Rupture of 48-Inch (1.22-m) X65 Steel Pipe

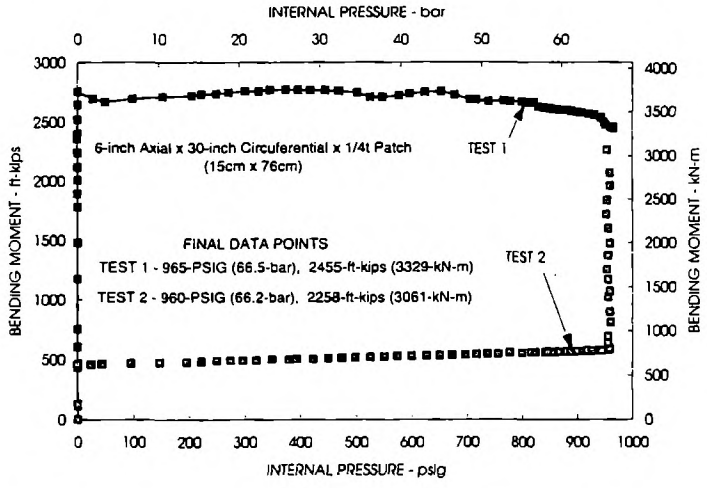

Figure 7: Internal Pressure Versus Bending Moment for Tests 6 and 7

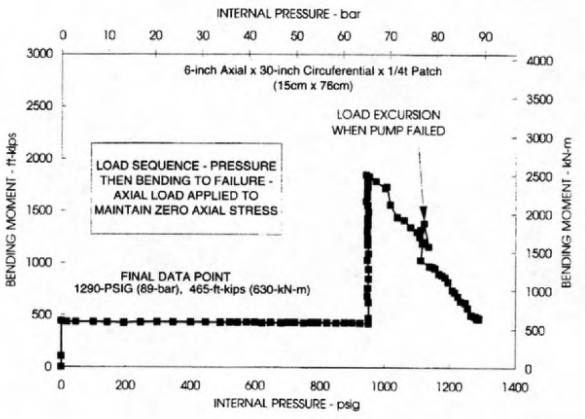

Figure 8: Specimen 8 - Internal Pressure Versus Bending Moment

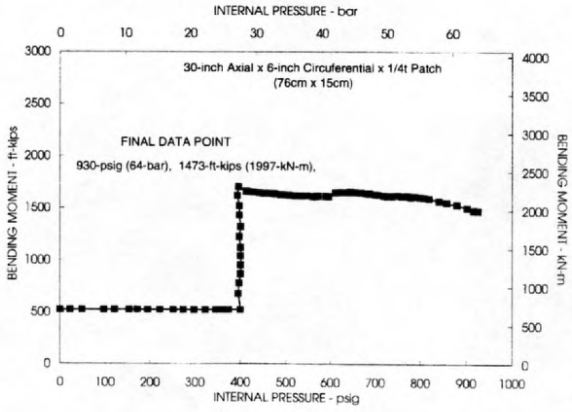

Figure 9: Specimen 9 - Internal Pressure Versus Bending Moment

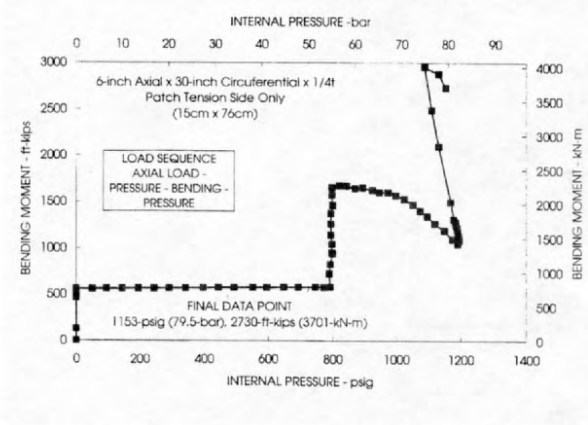

Figure 10: Specimen 10 - Internal Pressure Versus Bending Moment

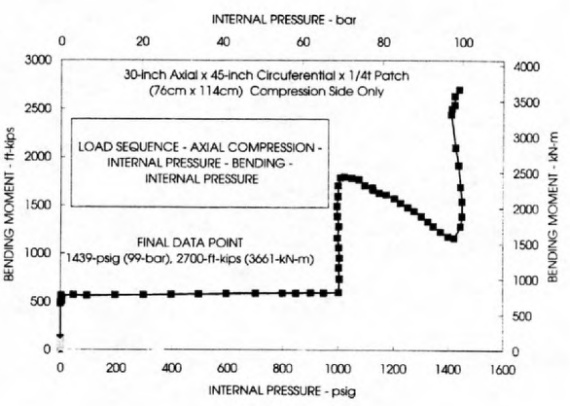

Figure 11: Specimen 11 - Internal Pressure Versus Bending Moment

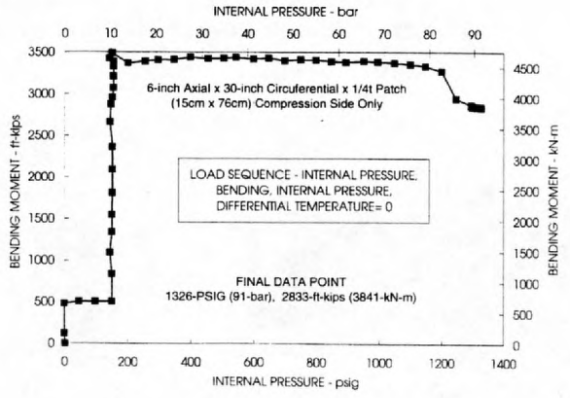

Figure 12: Specimen 12 - Internal Pressure Versus Bending Moment

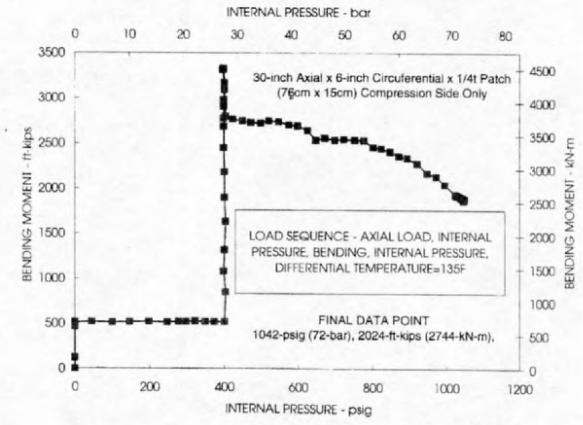

Figure 13: Specimen 13 - Internal Pressure Versus Bending Moment